

# The topology associated to cusp singular points

Konstantinos Efstathiou,<sup>a</sup> Andrea Giacobbe<sup>b</sup>

*Nonlinearity* **25**, 3409–3422 (2012) doi:[10.1088/0951-7715/25/12/3409](https://doi.org/10.1088/0951-7715/25/12/3409)

## Abstract

In this article we investigate the global geometry associated to cusp singular points of two-degree of freedom completely integrable systems. It typically happens that such singular points appear in couples, connected by a curve of hyperbolic singular points. We show that such a couple gives rise to two possible topological types as base of the integrable torus bundle, that we call pleat and flap. When the topological type is a flap, the system can have non-trivial monodromy, and this is equivalent to the existence in phase space of a lens space compatible with the singular Lagrangian foliation associated to the completely integrable system.

**Keywords:** completely integrable systems, bifurcation diagrams, cusp singularities, monodromy.

**MSC:** 55R55, 37J35

**PACS numbers:** 02.40.Vh, 02.40.Xx, 02.40.Yy

## 1 Introduction

### 1.1 Setup: completely integrable systems, singularities and unfolded momentum domain.

A two-degree of freedom completely integrable Hamiltonian system is a map  $f = (f_1, f_2)$ , from a four-dimensional symplectic manifold  $M$  to  $\mathbb{R}^2$ , with compact level sets, and whose components  $f_1$  and  $f_2$  Poisson commute [1, 3]. We will assume throughout the article, that the manifold  $M$  and the function  $f$  are real analytic. It is well known, see [1], that the regular level sets of such maps are disjoint unions of smooth 2-tori  $T^2$  and thus form a  $T^2$  bundle in phase space. Furthermore, it is possible to define an affine variety  $A$ , a map  $\tilde{f} : M \rightarrow A$ , and a projection  $\pi : A \rightarrow \mathbb{R}^2$ , such that the regular level sets of  $\tilde{f}$  are the connected components of the level sets of  $f$  and  $f = \pi \circ \tilde{f}$ , that is, the following diagram commutes, see [25].

$$\begin{array}{ccccc} & & f & & \\ & \curvearrowright & & \curvearrowleft & \\ M & \xrightarrow{\tilde{f}} & A & \xrightarrow{\pi} & \mathbb{R}^2 \end{array}$$

The affine variety  $A$  is called the *unfolded momentum domain*, and is a covering  $\pi : A \rightarrow \mathbb{R}^2$  of the *momentum domain* —the image of  $f$ — branched along the critical values of  $f$ . If  $x$  is an attained regular value of  $f$ , then there is a neighborhood  $U$  of  $x$  such that, above  $U$ , the variety  $A$  is a stack of open sets diffeomorphic to  $U$ , with as many components as those of  $f^{-1}(x)$ . The sets in such stacks join above the critical values of  $f$  according to rules that depend on the type of critical value. Thus the non-trivial topology of the unfolded momentum domain, and the geometry of the torus bundle, are due to the presence of singularities of the completely integrable system, see [12, 3].

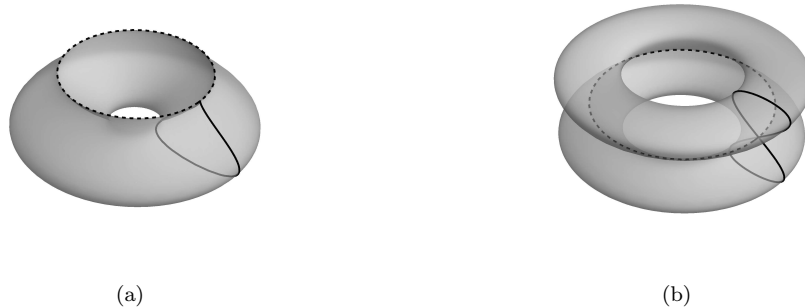


Figure 1: Singular fibers: (a) cuspidal torus, and (b) bitorus. The dashed lines represent the singularities of the fibers. These singularities are critical points of  $f$ .

## 1.2 Cusp singularities.

The singularity we plan to investigate is called a *cusp singularity*. Cusp singularities have been originally studied by the Russian mathematical school [18, 19, 20, 21, 17, 2], and were later revisited for investigations in semiclassical analysis [9] and in relation to the geometrical phenomenon of bidromy [11]. If  $p$  is a cusp singular point of  $f$  and  $c = f(p)$  is the corresponding *cusp critical value*, then the fiber  $C = f^{-1}(c)$  is a *cuspidal torus*. The cuspidal torus can be described as the product of a topological circle that has exactly one cusp singularity and a smooth circle, see Figure 1(a). The set of cusp singular points on  $C$  forms a smooth circle.

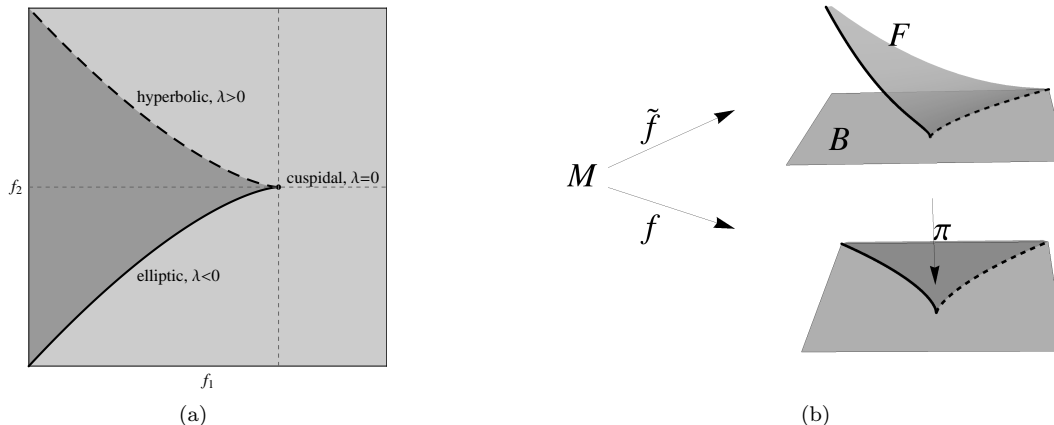


Figure 2: (a) The local bifurcation diagram of a cusp singularity and (b) its associated unfolded momentum domain. The two component region is represented by the darker gray shade.

From a cusp critical value  $c$  there originate two curves of critical values of  $f$ , one of elliptic and one of hyperbolic type, see Figure 2(a). The  $f$ -preimage of each hyperbolic critical value is a bitorus, depicted in Figure 1(b), while the  $f$ -preimage of each elliptic critical value consists of two disjoint components—a smooth circle  $S^1$  and a smooth torus  $T^2$ . The two curves of critical values originating from  $c$  separate an open neighborhood  $U$  of  $c$  in two regions of regular values. For each regular value  $v$  in the lighter shaded region  $\mathcal{R}_1$  of Figure 2(a) the fiber  $f^{-1}(v)$  is a smooth torus. On the other hand, the fiber above each regular value in the darker shaded region  $\mathcal{R}_2$  is the disjoint union of two smooth tori.

The topology of the unfolded momentum domain  $A$  in the  $\pi$ -preimage  $\pi^{-1}(U)$  of the neighborhood  $U$  of the cusp singularity  $c$  is depicted in Figure 2(b). Since fibers over elliptic critical values and regular values in  $\mathcal{R}_2$  consist of two disjoint components we conclude that the  $\pi$ -preimage of such values are two

disjoint points in  $A$ , and in particular that  $A$  is two-sheeted over such values. Moreover, the  $\pi$ -preimage of an elliptic critical value consists of a regular (interior) point of  $A$  corresponding to a smooth  $T^2$  and a singular (boundary) point of  $A$  corresponding to a smooth  $S^1$ . The sheet of  $\pi^{-1}(\mathcal{R}_2)$  that contains those singular points of  $A$  will be called the *local flap of  $c$* , and denoted by  $F$ . The other sheet of  $\pi^{-1}(\mathcal{R}_2)$  together with the  $\pi$ -preimage of  $\mathcal{R}_1$  will be called the *local base of  $c$* , and denoted by  $B$ . The intersection  $\bar{F} \cap \bar{B}$  of the closures of these sets forms the curve  $\ell$  that contains the cuspidal critical value  $c$  and the family of hyperbolic critical values connected to  $c$ . The regular component of the boundary of  $F$  will be called *free boundary*.

### 1.3 The problem and our results.

The way such a local picture contributes to the global bifurcation diagram of  $f$  is a complicated combinatorial problem, but there are two typical situations that often appear in applications and that we plan to discuss here. Cusp singularities often occur in pairs and, in such event, are typically joined either through their curve of elliptic critical values, like in Clebsh system [7], Manakov's top [23], Sretenskiĭ system [28] and Rubanovskiĭ system [4], or through their curve of hyperbolic critical values which is the case we investigate in this paper.

In Section 3 we show that in this second case the corresponding unfolded momentum domain can be of two different topological types, represented in Figure 3, that we call *pleat* and *flap*. Unfolded momentum domains with flap topology appeared in the physics literature in association with supercritical Hopf bifurcations [14] and with the phenomenon of *island monodromy* [14, 29], while unfolded momentum domains with pleat topology are related to Hamiltonian swallowtails [?, 13].

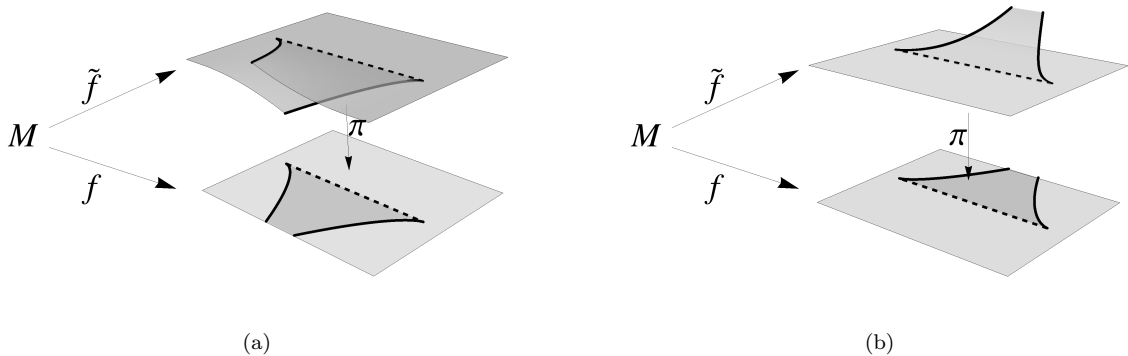


Figure 3: Two examples of unfoldings of bifurcation diagrams. The two unfolded momentum domain pictured are what we call (a) pleat and (b) flap. Thick lines (both solid and dashed) represent critical values. Solid thick lines represent the image of elliptic singularities while dashed thick lines represent the image of hyperbolic singularities.

The different topologies arise from the two different ways in which the local unfolded momentum domain near the two cusps can be glued together. Furthermore, the two cases can be analytically distinguished by comparing the sign of a third derivative at the cusp critical points. It turns out that the topology of the fibration of the phase space defined by  $f$  is uniquely determined if the unfolded momentum domain has pleat topology, see [13], while in the case of flap topology, the geometry of the fibration is more complicated. In Section 4 we confirm the fact that flap topologies can give rise to both, trivial and non-trivial monodromy (this fact has been discussed on examples in [11]), and we link this fact to the existence of a lens space  $L(k, 1)$ , compatible with the fibration, whose characterizing  $k$  is precisely the monodromy.

## 2 Cusp singularities

### 2.1 Analytic structure of cusp singularities.

As stated in the Introduction, we plan to describe the topology and the algebraic topology associated to couples of cusp singularities appearing in the theory of completely integrable systems. We begin by giving the definition of cusp singularities. To this effect we briefly recall that, given a two degree of freedom completely integrable system, the critical points are the points  $p$  in  $M$  such that the differential  $Df_p$  has rank less than two. Critical values are images of critical points. At a critical point, it is possible to define the *quadratic differential*  $D^2f_p$ , that is a quadratic form on the kernel of the differential  $Df_p$  with values in the co-kernel of  $Df_p$  [5]. Observe that whenever  $p$  is a critical point of rank 1, then the quadratic differential is a quadratic form from  $\mathbb{R}^3$  to  $\mathbb{R}$ . Moreover, the Poisson commutation of the components of  $f$  implies that there is always a vector in the kernel of  $D^2f_p$ , which hence has rank at most two. The non-degenerate cases, when  $\text{rank}(D^2f_p) = 2$ , can be separated into those in which  $D^2f_p$  has signature  $(0, +, +)$  or  $(0, -, -)$ , which correspond to elliptic singularities, or those in which  $D^2f_p$  has signature  $(0, +, -)$ , which correspond to hyperbolic singularities [3]. The simplest degenerate case, in which the quadratic differential has rank 1, is known as cusp singularity [9].

**Definition 1** *Given an integrable system  $f = (f_1, f_2)$ , a cusp singularity is a point  $p$  in the phase space such that the differential  $Df_p$  has rank 1, the quadratic differential  $D^2f_p$  has rank 1, and there exists a vector  $v \in \ker D^2f_p$  such that  $v^3f \neq 0$  (with  $v^3f$  we mean the third derivative of  $f$  along the tangent vector  $v$  at  $p$ ).*

What kind of singular fibers surround a cusp singularity? The local answer to this question can be obtained by means of a local normal form of the function  $f$ , see also [15].

**Proposition 2** *If  $p$  is a cusp singularity of  $f$  then there is a neighborhood  $U$  of  $p$  and (non-symplectic) coordinates  $q_1, p_1, q_2, p_2$  in  $U$  so that the restriction of the integrable fibration associated to  $f$  is locally given by the map  $f_{\text{local}} : (q_1, p_1, q_2, p_2) \mapsto (q_1, q_1p_2 + q_2^2 + p_2^3)$ .*

**Proof** Since  $\text{rank } Df_p = 1$  we can apply Caratheodory's theorem to obtain symplectic coordinates  $q_1, p_1, q_2, p_2$  with  $f_1 = q_1$  and  $f_2 = f_2(q_1, q_2, p_2)$ . Then  $f$  can be brought to the form  $f_{\text{local}}$  through coordinate transformations of the form  $(q_1, q_2, p_2) \mapsto (\phi(q_1), \psi_1(q_1; q_2, p_2), \psi_2(q_1; q_2, p_2))$  and coordinate transformations in the image of  $f$ , see [24] (Theorem V.5.4). Furthermore, the rescaling  $p_1 \mapsto p_1/\phi'(q_1)$  ensures that  $\{q_1, p_1\} = 1$ . Finally, note that  $\{q_1, q_2\} = \{q_1, p_2\} = 0$ .  $\square$

### 2.2 Local structure at a cusp singularity.

It follows from Proposition 2 that the set of critical points of  $f$  in the neighborhood  $U$  of the cusp singularity  $p$  is parameterized by  $(\mu, \lambda) \mapsto (-3\lambda^2, \mu, 0, \lambda)$  with  $(\mu, \lambda)$  defined in an open neighborhood of 0. Therefore the set of critical points in  $U$  is a smooth manifold. The image of these critical points under  $f$  give the critical values of  $f$  in the neighborhood  $f(U)$  of  $f(p)$  which are parameterized by  $c_\lambda : \lambda \mapsto (-3\lambda^2, -2\lambda^3)$  and form a cusp. Assuming that no other critical points exist in the saturation of  $U$  by fibers of  $f$  we conclude that  $c_\lambda$  describes the full set of critical values in  $f(U)$ . We denote by  $C_\lambda$  the preimage in phase space of  $c_\lambda$ . The intersections  $C_\lambda \cap U$  are defined in coordinates  $q_1, p_1, q_2, p_2$  by the equations

$$q_1 = -3\lambda^2, \quad -3\lambda^2p_2 + q_2^2 + p_2^3 = -2\lambda^3.$$

Thus, for  $\lambda = 0$  the set  $C_\lambda \cap U$  is the *cuspidal set*  $q_1 = 0, q_2^2 = -p_2^3$ ; for  $\lambda < 0$  it is a *bitoric set*; and for  $\lambda > 0$  it is an *elliptic set*. These sets are represented in Figure 4, and they trivially extend in the  $p_1$  direction.

**Remark.** Note that there are two cusps in different spaces. In the phase space, the local critical fiber  $C_0 \cap U$  is the product of a cusp with an open interval. In the image of  $f$  the family of critical values  $c_\lambda$  is also a cusp.

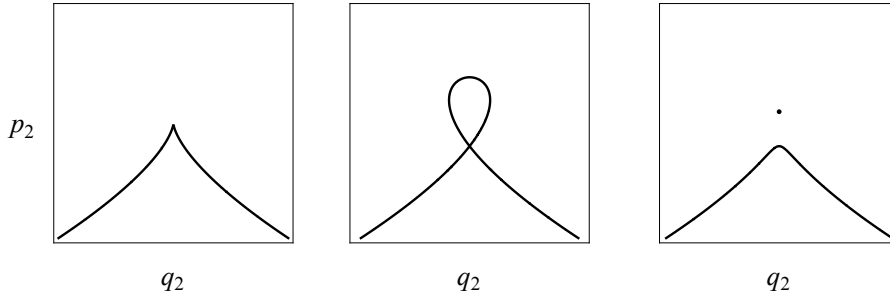


Figure 4: From left to right: intersections of the cuspidal torus, the bitorus, and the disjoint union of a torus and a circle with the  $p_1 = 0$  plane in a neighborhood of the cusp singular point to form respectively a cuspidal set, a bitoric set and an elliptic set, cf. Figure 5, left. In the elliptic case the critical points lie on an isolated line that intersects the  $p_1$ -plane in a point.

### 2.3 Semi-local structure at a cusp singularity.

A precise statement can be made concerning not only the topology of each level set  $C_\lambda$ , but also the structure of the Lagrangian fibration defined by  $f$  in a saturated neighborhood of a cusp singular point.

**Proposition 3** *Consider a cusp singular point  $p$  of  $f$  and assume that a saturated neighborhood of  $p$  contains no critical points of  $f$  other than those connected by the flows of  $X_1, X_2$  to the singularities given by  $f_{\text{local}}$  of Proposition 2. Then a saturated neighborhood of  $p$  is topologically the direct product of  $S^1$  with a 3-dimensional fibered space. The latter is obtained from the local fibration given by  $f_{\text{local}}$  by glueing together the two endpoints of each non-compact level set (see Figure 5). A saturated neighborhood of a hyperbolic singular point in the one-parametric family arising from the cusp singularity is topologically homeomorphic to the portion of the previous foliation with  $f_1 > 0$ .*

**Proof** Since  $f$  is assumed to be a proper map, its fibers are compact. One can always choose a function  $f_1$  for which  $df_1$  and thus  $X_1$  does not vanish at  $p$ . Hence, the cusp singularity  $p$  belongs to a 1-dimensional manifold of singularities of the same type which, due to compactness, must be a circle. The function  $f_1$  is hence non-critical on this circle, and thus also in a neighborhood of the circle. Using the Hamiltonian flows of  $f_1$  and  $f_2$  we conclude that  $df_1$  is never zero in a saturated neighborhood of  $p$ .

Consider now a three-dimensional local surface of section  $\Sigma$  of  $X_1$  at  $p$  (in the local non-symplectic coordinates is  $\Sigma = \{p_1 = 0\}$  and  $X_1 = \partial_{p_1}$ ). The local expression of Proposition 2 implies that the level sets of the components of  $f$  in  $\Sigma$  are those depicted in Figure 5 left. The common level-sets of  $f$  possess an orientation, given by the projection along  $X_1$  of the vector field  $X_2$ .

The Poincaré map  $\phi$  from  $\Sigma$  to itself defined by the flow of  $X_1$  preserves each stratum, where here a stratum is a connected component of the intersection of an  $\mathbb{R}^2$  orbit spanned by the flows of  $X_1, X_2$  with the local Poincaré surface of section  $\Sigma$ . In the case of the cuspidal level set the local strata are three, the fixed point  $p$  and the two open intervals that at one side end at  $p$ . In the case of bitoric sets the local strata are 4, the degenerate point, the two open intervals that at one side end at the degenerate point and the loop with both sides ending at the degenerate point. The preservation of each of these strata does not follow directly from conservation of  $f_2$  but relies also on the preservation of  $X_2$  (since it commutes with  $X_1$ ) and on the continuous dependence of solutions on initial conditions. Letting  $\Sigma'$  be the subset of points of  $\Sigma$  whose image under the Poincaré map  $\phi$  still belongs to  $\Sigma$ , one can observe that  $\tilde{\Sigma}'$ , the saturation of  $\Sigma'$  under the flow of  $X_1$ , being isomorphic to the gluing of  $B \times [0, 1]$  with  $B$  a 3-ball, along the boundaries  $B \times \{0\}$  and  $B \times \{1\}$ , retracts to a circle which we can choose to be the circle of cusp singularities.

Every point  $x \in \Sigma'$  belongs to a unique cycle  $\gamma_x$  composed by the flow of  $X_1$  up to the first return time and the interval connecting  $x$  to  $\phi(x)$  in the stratum. The cycle  $\gamma_x$  depends continuously on the point

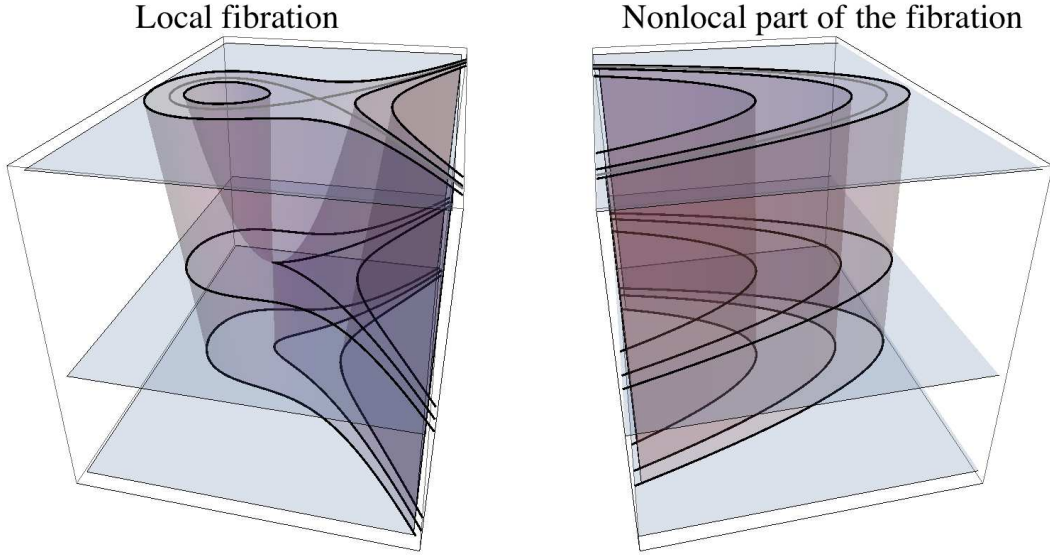


Figure 5: A Poincaré surface of section for the vector field  $X_1$  with level sets of the function  $f_1$  (horizontal planes) and the function  $f_2$ . The fibers of  $f$  that contain this set are topologically compact. This fact is pictorially represented by adding the intervals that connect endpoints of the same component. The section consists in this picture cross-multiplied with  $S^1$ . The subset associated to  $f_1 > 0$  is that whose vertical component is above the singular point. The lighter figure 8 curve corresponds to a bitorus.

$x$ , because of smoothness of the flow of  $X_1$  and smooth dependence of the image of the Poincaré map. Observe that the cycle  $\gamma_x$  is simply continuous, but it possibly is non-differentiable at two points. As  $x$  approaches  $p$  the cycle  $\gamma_x$  approaches the cycle of cuspidal critical points through  $p$ . Let  $\vartheta$  be a canonical 1-form defined in  $\Sigma'$  (such 1-form exists because the topology of the space is  $S^1$  times a 3-dimensional ball), the function  $J(x) = \frac{1}{2\pi} \int_{\gamma_x} \vartheta$  can be extended to a saturated neighborhood of the cuspidal point by using the fact that it is constant along the level sets of  $f$ , and is the Hamiltonian of a circle action in such neighborhood with no isotropy. The existence of such a circle action in a saturated neighborhood of cuspidal tori and bitori can also be found in [30].

Reducing such neighborhood under the circle action  $X_J$  and using the reduced flow of  $X_2$  one obtains a space whose topology and whose structure of  $f$  level sets is the one of Figure 5 left glued to the space of Figure 5 right. Reconstruction of the  $S^1$  action gives a manifold isomorphic to  $\Sigma' \times S^1$ . In fact  $\tilde{\Sigma}'$  could be isomorphic to the quotient of  $\Sigma' \times S^1$  under a finite group action fixing the cusp singularity, but the structure of the foliation near such singularity forces such group to be at most  $\mathbb{Z}_2$ , while this latter possibility can be discarded because of the preservation of  $X_2$ .

The description of the local structure at hyperbolic singular points near the cusp singular points is included in the previous discussion. It will not change as the hyperbolic singularity moves to neighboring hyperbolic singular points because the local description of hyperbolic singularities does not allow a change of the isotropy.  $\square$

A consequence of this description is that the cuspidal set belongs to a cuspidal torus, that is a non-smooth  $T^2$  which contains a circle of singular points and whose intersection with a plane transverse to this circle is locally a cusp, while the elliptic set belongs to a level set isomorphic to the disjoint union of a circle  $S^1$  with a regular two torus  $T^2$ , and finally the bitoric set belongs to a bitorus, see [26].

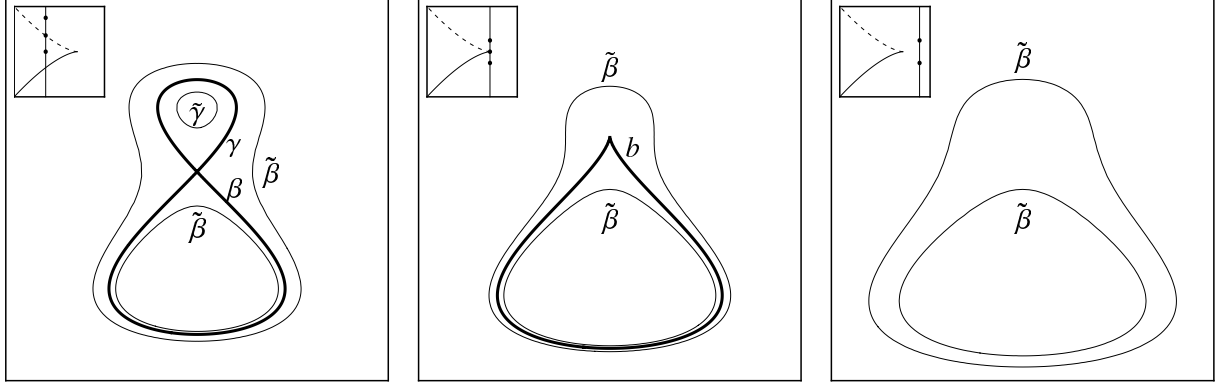


Figure 6: Homology cycles for fibers in a neighborhood of a cusp singularity. Here the intersections of fibers with the Poincaré surface of section  $\Sigma$  are shown and the homology cycles supported by these intersections are marked. Singular level sets (bitorus, cuspidal torus) are drawn with thicker lines. For each fiber the corresponding projection to the base space of the fibration is shown. Note that in the leftmost panel, the two components denoted by  $\tilde{\beta}$  and  $\tilde{\gamma}$  inside the bitorus project under  $f$  to the same point in the interior of the cusp, although they project under  $\tilde{f}$  to different points in the unfolded momentum domain:  $\tilde{\gamma}$  projects under  $\tilde{f}$  inside the flap while  $\tilde{\beta}$  projects outside the flap, cf. Figure 2.

## 2.4 Homology cycles and their parallel transport in a neighborhood of a cusp singularity

Given the description of a saturated neighborhood of a cusp singularity as a direct product it is possible to give a full description of the homology cycles on fibers in such neighborhood and their parallel transport between different fibers (the reason for dealing with first homology group and not first homotopy group is discussed in [16]). In order to facilitate the discussion we depict in Figure 6 the intersections of fibers in the neighborhood of the cusp with a Poincaré surface of section. The full fiber is then reconstructed as the direct product of these intersections with  $S^1$ , where this  $S^1$  is provided by the circle action defined in the saturated neighborhood of the cusp, see Proposition 3.

The regular fibers of  $\tilde{f}$  are smooth two dimensional tori  $T^2$  and their first homology group, which is isomorphic to  $\mathbb{Z}^2$ , is generated by two cycles. One cycle, that we call  $\tilde{\alpha}$ , can be chosen as associated to the circle action, and is supported by the circle  $S^1$  taking part in the direct product. This cycle is well defined on all fibers. For regular fibers that project under  $\tilde{f}$  outside the flap, the second cycle is denoted by  $\tilde{\beta}$  and is supported by the intersection of the regular fiber with the Poincaré section as shown in Figure 6. For regular fibers that project under  $\tilde{f}$  inside the flap, the second cycle is denoted by  $\tilde{\gamma}$  and is again supported by the intersection of the regular fiber with the Poincaré section.

The cuspidal torus  $C_0$  also has first homology group which is isomorphic to  $\mathbb{Z}^2$ , and is generated by two cycles that we denote by  $a$  and  $b$ . The cycle  $a$  is again associated to the circle action and is parallel transported to  $\tilde{\alpha}$ . The cycle  $b$  is supported by the intersection of the cuspidal torus with the Poincaré section shown in Figure 6.

The bitori (denoted by  $C_\lambda$  with  $\lambda < 0$  in the local analytic description of Section 2B) have first homology group which is isomorphic to  $\mathbb{Z}^3$ , and is generated by three cycles  $\alpha$ ,  $\beta$ ,  $\gamma$ . The cycle  $\alpha$  can be chosen to be the cycle associated to the circle action. The set of regular points of a bitorus has two connected components; calling *lobe* of a bitorus each of the closure of such components, the above analysis shows that, when approaching the cuspidal torus ( $C_0$  in the local description), one of the lobes of the bitori shrinks onto the circle of singular points of the cuspidal torus. We call that lobe a (*local*) *vanishing lobe*. Given these names, we can choose the cycle  $\beta$  to be represented by a circle that lies in the non-vanishing lobe and choose the cycle  $\gamma$  to be represented by a circle that lies in the vanishing lobe.

The cycle  $\gamma$  can be chosen so that it is cobordant to 0 in the cuspidal torus  $C_0$ .

The description of cycles in terms of curves on the Poincaré surface of section allows to determine a cobordism relation among such cycles (sometimes referred to as *parallel transport*). Along a path that joins a regular fiber in the local base  $B$  to the  $f$ -image of the cuspidal torus  $C_0$ , the cycles  $\tilde{\beta}$  are cobordant to  $b$  while the cycles  $\tilde{\gamma}$  are cobordant to zero. Furthermore, along a path that joins a regular fiber in  $B$  to a bitorus on the curve  $\ell$  of hyperbolic and cusp critical values, the cycle  $\tilde{\beta}$  is cobordant to  $\beta$  with a cobordism that projects to an interval ending in  $\ell$  from the flap side, while it is cobordant to  $\beta + \gamma$  with a cobordism that projects to an interval ending in  $\ell$  from the other side.

### 3 Pleats and flaps

#### 3.1 Two possible topologies of the unfolded momentum domain.

We can now focus on the problem of pairs of cuspidal singularities that we described in the Introduction. Let us assume to be given a 2 degrees of freedom completely integrable system with a line segment  $\ell$  of critical values, parameterized by  $[0, 1] \ni s \mapsto c_s \in \mathbb{R}^2$ , so that the endpoints  $c_0$  and  $c_1$  are cusp critical values while the interior points  $c_s$  for  $s$  in  $]0, 1[$  are hyperbolic critical values. As already recalled, the level sets  $C_s = f^{-1}(c_s)$  for  $s$  in  $\{0, 1\}$  are cuspidal tori, while the level sets  $C_s = f^{-1}(c_s)$  for  $s$  in  $]0, 1[$  are bitori [3, 30, 8].

As  $s$  approaches 0 or 1 one lobe of the bitorus  $C_s$  vanishes. In this setup, only two possible things can happen: either the lobe that vanishes when approaching the cuspidal torus  $C_0$  is the same that vanishes when approaching the cuspidal torus  $C_1$ , or not.

The topology of the unfolded momentum domain can be deduced from this description in the following way: consider the local unfolded momentum domain—depicted in Figure 2—of a saturated neighborhood of each cusp critical value  $c_0$  and  $c_1$ . The topology of the unfolded momentum domain in a neighborhood of the hyperbolic line  $\ell$  is obtained by glueing together these two local unfolded momentum domains. Each of the local unfolded momentum domains has a local flap  $F_0, F_1$  and a local base  $B_0, B_1$ , each containing the critical values  $c_0$  and  $c_1$  respectively. The local flaps must be on the same side of the hyperbolic line, because the regular values whose preimage has two components must match. Recalling that the free boundary is the regular part of the boundary of the local flap, we observe that there are once again two possibilities for glueing: either the free boundary of  $F_0$  is glued to the free boundary of  $F_1$  and the boundary of  $B_0$  to the boundary of  $B_1$ , or the free boundary of  $F_0$  is glued to the boundary of  $B_1$  and the free boundary of  $F_1$  is glued to the boundary of  $B_0$ . The first case corresponds to the *flap topology* around  $\ell$  while the second case to the *pleat topology* (see Figure 3). Recalling that the vanishing lobe corresponds to fibers in the local flap we conclude that in the case of the flap topology it is the same lobe that vanishes at the two ends of  $\ell$  while in the case of the cusp topology one lobe vanishes at one end and the other lobe vanishes at the other end. Thus we have the following result.

**Proposition 4** *In a 2 degree of freedom completely integrable Hamiltonian system with a line segment  $\ell$  of critical values, so that the endpoints are cusp critical values while the interior points are hyperbolic critical values, the unfolded momentum domain  $A$  in an open neighborhood of  $\ell$  can have one of the following two topological types: the pleat topology as in Figure 3(a), or the flap topology as in Figure 3(b).*

#### 3.2 Associated analytic description.

The argument given above has an analytic counterpart, that can be also used to discriminate one case from the other. Denote by  $d_s, s \in [0, 1]$  any smooth 1-parameter family of singular points with  $d_s \in C_s$  for each  $s \in [0, 1]$ . At the cusp singularities  $d_0$  and  $d_1$ , the completely integrable system  $f$  has rank 1 and its quadratic differential  $D^2f$  is a quadratic form defined in  $\mathbb{R}^3$  and taking values in  $\mathbb{R}$  with a 2-dimensional null-space. From the cusp singular value, departs a thread of rank 1 singularities  $d_s, s \in ]0, 1[$  of hyperbolic type, at which the quadratic differential of  $f$  has signature  $(0, +, -)$ .



In the local normal form coordinates  $q_1, p_1, q_2, p_2$  introduced for  $d_0$  in Proposition 2, the vector field  $\partial_{p_2}$  points in the direction of the vanishing lobe and is in the negative space of the quadratic differential of  $f$ . Prolonging such vector field to a vector field  $V$  defined along the line of hyperbolic critical points  $d_s$  so that  $V(d_s)$  belongs to the negative space of the quadratic differential  $D^2 f_{d_s}$  for every  $s$  in  $]0, 1[$ , one can approach the other cusp singular point  $d_1$ . In a neighborhood of  $d_1$ , it is possible to introduce using Proposition 2 local adapted coordinates  $x_1, y_1, x_2, y_2$  satisfying the same conditions as coordinates  $q_1, p_1, q_2, p_2$ . In such coordinates, the completely integrable system is given by two functions  $f = (x_1, x_1 y_2 + x_2^2 + y_2^3)$ .

The shrinking lobes of the bitori  $C_s$ , when  $s$  is close to one, are those in the  $y_2$  positive plane. The vector  $V(d_s)$  must be in the negative space of the quadratic differential of  $f$ , and it belongs either to the same component of  $\partial_{y_2}$  or to the other component. This discriminates the two cases. In particular, the first case corresponds to the flap topology while the second case to the pleat topology.

### 3.3 Circle action in a saturated neighborhood of hyperbolic line.

One fact that we will find useful can be easily deduced from the literature [30]. Whatever the topology of the unfolded momentum domain may be, one can always find a neighborhood  $V$  of the curve  $\ell$  such that the saturated neighborhood  $f^{-1}(V)$  of the hyperbolic singularities admits a unique Hamiltonian  $S^1$  action.

**Proposition 5** *A saturated neighborhood of  $\ell$  admits a unique Hamiltonian circle action.*

**Proof** Theorem 1.2 in [30], rephrased in our case, states that in a neighborhood of an orbit of dimension 1 which is not non-degenerate elliptic type and which belongs to a level set of  $f$  which is at most 2-dimensional, admits a unique circle action. Since hyperbolic and cusp singular points of the integrable system at hand satisfy the assumptions of the Theorem, it follows that every point  $c_s$ , for  $s$  in  $[0, 1]$ , has a neighborhood whose preimage admits a unique Hamiltonian circle action. The statement follows from the uniqueness of these circle actions.  $\square$

## 4 Flaps and monodromy

### 4.1 Description of a saturated neighborhood of a flap: the appearance of lens spaces.

Let us assume, from now on, to be in the case in which the unfolded momentum domain has flap topology, and let  $\ell$  be the line we described in Subsection 3.1. For a point  $c_s \in \ell^\circ$  the preimage  $f^{-1}(c_s)$  is a bitorus—a singular set that consists of two non-smooth tori  $T^2$  transversally joined along a circle  $S^1$ . For a point  $c_s \in \partial\ell$  the preimage  $f^{-1}(c_s)$  is a cuspidal torus where the cusp points form a  $S^1$ . Thus for all  $c_s \in \ell$  there is in the fiber  $f^{-1}(c_s)$  a distinguished  $S^1$  which is the set of critical points of  $f$  in  $C_s = f^{-1}(c_s)$ . This implies that the set  $O$  of critical points of  $f$  in  $L = f^{-1}(\ell)$  is a cylinder  $S^1 \times I$ , where  $I = [0, 1]$ .

Furthermore, the preimage  $L = f^{-1}(\ell)$  is a singular set in  $M$ . Consider a point  $c_s$  that moves along  $\ell$ . When  $s$  belongs to  $]0, 1[$  the fiber  $f^{-1}(c_s)$  consists of two lobes, but when either  $s = 0$  or  $s = 1$  one of the lobes—the same for both cases—shrinks to the singular  $S^1$  of the cuspidal torus, while the other lobe becomes the cuspidal torus. Thus the set  $L$  can be described as the union of the set  $V$  of *vanishing lobes*, and the set  $S$  of *non-vanishing lobes*, with  $V \cap S = O$ .

The set  $S$  of non-vanishing lobes is a  $T^2$  bundle over the contractible line  $\ell$ . Therefore,  $S$  is homeomorphic to  $T^2 \times I$ . We now investigate the structure of  $V$ . Consider a decomposition of  $\ell$  in two closed sets  $\ell_1$  and  $\ell_2$  such that  $\ell_1 \cap \ell_2 = \{c\}$ , with  $c \in \ell^\circ$ . Then the sets  $V_1$  and  $V_2$  of vanishing lobes over  $\ell_1$  and  $\ell_2$  respectively are both homeomorphic to a solid torus and  $V = V_1 \cup V_2$  while  $V_1 \cap V_2$  is homeomorphic to  $T^2$ . It follows that the set of vanishing lobes  $V$  is a lens space  $L(p, q)$  [6] constructed by glueing  $V_1$  and  $V_2$  along their common  $T^2$  boundary with a homeomorphism  $h : \partial V_1 \rightarrow \partial V_2$ . The existence of the one-parameter family of circles  $O$  that connects the central circle of  $V_1$  to the central

circle of  $V_2$  shows that the lens space is  $L(k, 1)$  with  $k \in \mathbb{N}$  (in our definitions  $0 \in \mathbb{N}$ , and when  $k = 0$  then  $L(0, 1) = S^2 \times S^1$ ). Note that the latter follows also from the existence on  $V$  of a  $S^1$  action without fixed points. This argument proves the following result.

**Proposition 6** *The preimage  $f^{-1}(\ell)$  consists of the set of vanishing lobes which is a topological lens space  $L(k, 1)$  with  $k \in \mathbb{N}$  and the set of non-vanishing lobes which is homeomorphic to  $T^2 \times I$ . The two sets are joined along the cylinder  $O = S^1 \times I$  of critical points of  $f$ .*

## 4.2 Monodromy around a flap

In this section we describe the role of monodromy in completely integrable systems whose unfolded momentum domains have flap topology. Recall that in this case there is in the unfolded momentum domain  $A$  a line  $\ell$  of hyperbolic and cuspidal critical values. The set  $\ell$  separates  $A$  into two parts: the flap  $F$ , and  $B = A \setminus \overline{F}$ . Both  $F$  and  $B$  are open in  $A$  and their common boundary is  $\ell$ . The fundamental group  $\pi_1(B)$  contains a path encircling  $\ell$ ; the monodromy of the torus bundle along that path can hence be non-trivial.

**Proposition 7** *Consider a 2 degree of freedom completely integrable Hamiltonian system  $f$  with a line segment  $\ell$  of critical values, so that the endpoints are cusp critical values while the interior points are hyperbolic critical values, and such that the unfolded momentum domain  $A$  in an open neighborhood of  $\ell$  has the flap topology. Then the type of lens space  $L(k, 1)$  topologically embedded in  $f^{-1}(\ell)$  determines the monodromy index  $k$  of the torus bundle along a path surrounding  $\ell$  up to a sign determined by the choice of orientations.*

**Proof** Recalling the discussion of Section 2 C, each bitorus  $C_s$ , with  $s \in ]0, 1[$ , has first homology group which is isomorphic to  $\mathbb{Z}^3$  and is generated by three cycles  $\alpha, \beta, \gamma$ . The cycle  $\alpha$  is associated to the circle action. The cycle  $\beta$  lies in the non-vanishing lobe  $T_S = C_s \cap S \simeq T^2$  and together with  $\alpha$  gives a basis for  $H_1(T_S) \simeq \mathbb{Z}^2$ . The cycle  $\gamma$  lies in the vanishing lobe  $T_V = C_s \cap V \simeq T^2$  and together with  $\alpha$  gives a basis for  $H_1(T_V) \simeq \mathbb{Z}^2$ . Since the closure of the vanishing lobes is a lens space  $L(k, 1)$ , the cycle  $\gamma$  can be chosen so that it is cobordant to 0 in the cuspidal torus  $C_0$  and is hence cobordant to  $k\alpha$  in the cuspidal torus  $C_1$ .

Consider now a covering of the hyperbolic line consisting of the neighborhoods  $U_0, \dots, U_n$ , with  $U_0$  a neighborhood of  $c_0$  and  $U_n$  a neighborhood of  $c_1$  small enough so that the structure of the foliation above them is that described in Proposition 3. Note that  $U_i$  for  $i \neq 0, n$  is separated by  $\ell$  to two regions: one that contains points in the double component region and that we denote by  $U_i^-$  and the rest that we denote by  $U_i^+$ .

In all  $U_i$ ,  $i = 0, \dots, n$ , one can choose a basis  $\alpha_i, \beta_i, \gamma_i$  for the bitori so that  $\beta_i$  belongs to the non-vanishing lobes,  $\gamma_i$  belongs to the vanishing lobes, and  $\alpha_i$  is defined by the  $S^1$  action.

Furthermore, a basis  $\tilde{\alpha}_i, \tilde{\beta}_i$  for regular tori over  $U_i$ ,  $i \neq 0, n$ , is defined in the following way. The cycle  $\tilde{\alpha}_i$  is always defined by the  $S^1$  action and is thus parallel transported to  $\alpha_i$  along any path that ends at a bitorus. For regular values in  $U_i^+$  we define  $\tilde{\beta}_i$  as the cycle that is parallel transported to  $\beta_i + \gamma_i$  along a path in  $U_i^+ \cup \ell_i$  where  $\ell_i = \ell \cap U_i$ . For regular values in  $U_i^-$  we define  $\tilde{\beta}_i$  as the cycle that is parallel transported to  $\beta_i$  along a path in  $U_i^- \cup \ell_i$ .

For  $U_0$  and  $U_n$  we make the same choices as described in Section 2.4. In particular, we choose the cycles  $\gamma_0, \gamma_n$  to be parallel transported along a path in  $\ell$  to the zero cycle in the corresponding cuspidal tori  $C_0$  and  $C_1$  respectively. Recall that in  $U_0$  the cycle  $\tilde{\beta}_0$  defined on a regular torus is parallel transported to  $\beta_0 + \gamma_0$  from one side of  $\ell$  and to  $\beta_0$  from the other side.

In the overlapping  $U_0^+ \cap U_1^+$ , the cycles  $\tilde{\alpha}_0, \tilde{\beta}_0$  can be expressed respectively as  $\tilde{\alpha}_1, \tilde{\beta}_1 + \lambda_{01}^+ \tilde{\alpha}_1$ , while in the overlapping  $U_0^- \cap U_1^-$  we have that  $\tilde{\alpha}_0, \tilde{\beta}_0$  can be expressed respectively as  $\tilde{\alpha}_1, \tilde{\beta}_1 + \lambda_{01}^- \tilde{\alpha}_1$ . On the other hand, also the cycles  $\alpha_0, \beta_0, \gamma_0$  can be expressed respectively as  $\alpha_1, a_{01}\beta_1 + b_{01}\gamma_1 + \lambda_{01}\alpha_1, c_{01}\beta_1 + d_{01}\gamma_1 + \mu_{01}\alpha_1$  in  $\ell_0 \cap \ell_1$ . The cobordism relation of cycles in the regular fibers with cycles in the singular fiber forces the identities

$$\begin{aligned}
\beta_1 + \gamma_1 + \lambda_{01}^+ \alpha_1 &= (a_{01} + c_{01})\beta_1 + (d_{01} + b_{01})\gamma_1 + (\lambda_{01} + \mu_{01})\alpha_1, \\
\beta_1 + \lambda_{01}^- \alpha_1 &= a_{01}\beta_1 + b_{01}\gamma_1 + \lambda_{01}\alpha_1.
\end{aligned} \tag{1}$$

It follows that  $a_{01} = 1 = d_{01}$ ,  $b_{01} = 0 = c_{01}$ ,  $\lambda_{01}^+ = \lambda_{01} + \mu_{01}$  and  $\lambda_{01}^- = \lambda_{01}$ . Proceeding with this process up to  $U_n$ , one can prove that the parallel transport of the cycle  $\tilde{\beta}_0$  around the hyperbolic line gives  $\tilde{\beta}_0 + (\mu_{01} + \cdots + \mu_{(n-1)n})\tilde{\alpha}_0$ .

One just needs to recall that the cycle  $\gamma_0$ , which is parallel transported to the zero cycle in the cuspidal torus  $C_0$ , is also parallel transported along  $\ell$  to the cycle  $\gamma_n + (\mu_{01} + \cdots + \mu_{(n-1)n})\alpha_n$  in the bitori close to the cuspidal torus  $C_1$ , with  $\gamma_n$  also homologous to zero. Being a lens space  $L(k, 1)$ , it follows that  $\mu_{01} + \cdots + \mu_{(n-1)n} = k$ , and this concludes the proof.  $\square$

**Remark.** Denote by  $F_0$  and  $F_1$  the two local boundaries of elliptic critical points of  $F$ . Consider a closed segment  $[0, 1] \ni t \mapsto \gamma(t) \in F$  with endpoints  $\gamma(0) \in F_0$  and  $\gamma(1) \in F_1$  and with  $\gamma(]0, 1[) \subset F^\circ$ . The preimages  $f^{-1}(\gamma(]0, 1/2[))$  and  $f^{-1}(\gamma(]1/2, 1[))$  are also solid tori, and the preimage  $f^{-1}(\gamma(]0, 1[))$  is the topological space obtained by glueing the two solid tori along their boundaries according to an automorphism of  $T^2$ . It follows that these too are lens space  $L(p, q)$ . Also in this case, the existence of a circle action without fixed points implies that we are dealing with lens spaces of type  $L(k, 1)$ . Moreover, all the lens spaces obtained so far, up to the singular one are all isomorphic.

**Remark.** Proposition 7 concerns the *absolute* monodromy around the line  $\ell$ , as we do not take into account in our arguments the orientations of the path in the momentum domain and of homology cycles on the fibres. Nevertheless, we expect that arguments like those in [10] can prove that *oriented* monodromy carries a sign which is positive, provided that positive orientations are chosen for the path and for the homology cycles. The lens space  $L(k, 1)$  does not carry a sign since  $L(k, 1)$  is isomorphic to  $L(-k, 1)$ . Therefore, the possibility that monodromy carries a sign implies a restriction on the possible embedding of the lens space in the fibration.

### 4.3 Existence and uniqueness

This subsection is based on suggestions of an anonymous referee concerning the application to the present problem of Fomenko's theory on Lagrangian foliations [3]. We owe to the referee most of the ideas and techniques that are briefly outlined here. Our Proposition 7 indicates that to every two-degree of freedom completely integrable system with a flap topology one can associate a natural number but does not prove that all natural numbers can be obtained, nor that such natural number uniquely determines the topology of a semiglobal neighborhood of the line  $\ell$  of hyperbolic singularities.

The bijection between  $k \in \mathbb{N}$  and the topology of semiglobal neighborhoods of the hyperbolic line  $\ell$  can be proven by a glueing argument (proposed by the referee). The topology of a saturated neighborhood  $U$  of the cusp singularity has been described accurately in Section 2. A semiglobal neighborhood of the hyperbolic line must be the glueing of two such neighborhoods  $U_1, U_2$  along the preimage of an interval that transversally intersects the line of hyperbolic singularities. Such preimage is  $S^1$  times a thick figure-of-eight open set. It turns out that, under appropriate choice of the reference cycles of the fibers, such glueing is uniquely defined up to a matrix that is a  $2 \times 2$  matrix of the form  $\begin{pmatrix} 1 & k \\ 0 & 1 \end{pmatrix}$ . This proves that there exist at least semiglobal models for this topological setup, and that the number  $k$  uniquely determines the topology.

We are left with the question of whether, for every natural  $k$ , there exists a completely integrable system with a flap, possessing monodromy  $k$  around the line of hyperbolic singularities. A model with  $k = 0$  can be found in [11], while models with  $k = 1$  are the easiest to find (see e.g. [14]). An example with  $k = 2$ , can be given in the phase space  $T^*S^2$ , choosing  $H = x_2 + (y_1^2 + y_2^2 + y_3^2)(y_1^2 + y_2^2 + y_3^2 - 3)$  as Hamiltonian and the angular momentum  $J = x_1y_2 - x_2y_1$  as other commuting function. We are not aware of any such examples with  $k \geq 3$ , but for  $k$  up to 4 it is presumably possible to construct examples in  $S^2 \times S^2$  (where we can produce a second example with  $k = 2$ ). For higher  $k$ , examples should be

found in appropriate connected sums of  $CP^2$ , by appropriately deforming their structure of almost toric manifolds [22].

## 5 Acknowledgements

A.G. has been partially supported by the University Research Project (PRA) CPDA081081/08, and wishes to thank H.W. Broer for inviting him to the University of Groningen. K.E. has been supported by the NDNS<sup>+</sup> research cluster of NWO (Dutch Scientific Organization) and wishes to thank F. Fassò for his invitation to the University of Padova. Both authors acknowledge useful discussions with B. Zhilinskiĭ and D. Sadovskii. We would also like to thank the referees of this work for their comments that noticeably improved the article.

## References

- [1] V.I. Arnol'd, *Mathematical Methods of Classical Mechanics*, Graduate Texts in Mathematics **60**, Springer-Verlag, New York, 2 edition, (1989), isbn:0387968903
- [2] A.V. Bolsinov, S.V. Matveev, A.T. Fomenko, Topological classification of integrable Hamiltonian systems with two degrees of freedom. List of systems of small complexity, *Russian Mathematical Surveys* **45/2**, 59–94 (1990), doi:10.1070/RM1990v045n02ABEH002344
- [3] A.V. Bolsinov, A.T. Fomenko, *Integrable Hamiltonian systems*, Chapman & Hall/CRC (2004), isbn:0415298059
- [4] A.V. Bolsinov, I. Basak, Bifurcation analysis of Rubanovskii system via bi-Hamiltonian approach, *International symposium on rare attractors and rare phenomena in nonlinear dynamics, Riga-Jurnala, Latvia*, 70–73 (2011)
- [5] T. Bröcker, *Differentiable germs and catastrophes*, Cambridge University Press, London Mathematical Society Lecture Note Series 17 (1975), isbn:0521206812
- [6] E.J. Brody, The topological classification of the lens spaces, *Annals of Mathematics*, **71/1**, 163–184 (1960), doi:10.2307/1969884
- [7] A. Clebsch, Über die bewegung eines korpers in einer flussigkeit, *Mathematische Annalen* **4/2**, 238–262 (1871),
- [8] Y. Colin de Verdière, S. Vũ Ngợc, Singular Bohr-Sommerfeld rules for 2D integrable systems, *Ann. Scient. Ec. Norm. Sup.* **36**, 1–55 (2003), doi:10.1016/S0012-9593(03)00002-8
- [9] Y. Colin de Verdière, Singular Lagrangian manifolds and semiclassical analysis, *Duke Mathematical Journal* **116/2**, 263–298 (2003), doi:10.1215/S0012-7094-03-11623-3
- [10] R.H. Cushman, S. Vũ Ngợc, Sign of the monodromy for Liouville integrable systems, *Annales Henri Poincaré* **3**, 883–894 (2002), doi:10.1007/s00023-002-8640-7
- [11] G. Dhont, B.I. Zhilinskiĭ, Classical and quantum fold catastrophe in the presence of axial symmetry, *Physical Review A* **78**, 052117 (2008), doi:10.1103/PhysRevA.78.052117
- [12] J.J. Duistermaat, On global action-angle coordinates, *Communications on Pure and Applied Mathematics* **33/6**, 687–706 (1980), doi:10.1002/cpa.3160330602
- [13] K. Efstathiou, D. Sugny, Integrable Hamiltonian systems with swallowtails, *Journal of Physics A: Math. Theor.* **43**, 085216 (2010), doi:10.1088/1751-8113/43/8/085216
- [14] K. Efstathiou, *Metamorphoses of Hamiltonian Systems with Symmetries*, Springer, Berlin Heidelberg New York, 2005, isbn:354024316X
- [15] A. Giacobbe, Infinitesimally stable and unstable singularities of 2-degrees of freedom completely integrable systems, *Regular and Chaotic Dynamics* **12/6**, 717–731 (2007), doi:10.1134/S1560354707060123
- [16] A. Giacobbe, Fractional monodromy: parallel transport of homology cycles *Differential Geometry and its Applications* **26**, 140–150 (2008), doi:10.1016/j.difgeo.2007.11.011
- [17] V.V. Kalashnikov, Typical integrable Hamiltonian systems on a four-dimensional symplectic manifold, *Izvesia: Mathematics* **62/2**, 49–74 (1998), doi:10.1070/IM1998v062n02ABEH000173

- [18] L.M. Lerman, Y.L. Umanskiĭ, Classification of four-dimensional integrable Hamiltonian systems and Poisson actions of  $\mathbb{R}^2$  in extended neighborhoods of simple singular points. I, *Sbornik: Mathematics* **183**/12, 141–176 (1992), doi:[10.1070/SM1994v077n02ABEH003454](https://doi.org/10.1070/SM1994v077n02ABEH003454)
- [19] L.M. Lerman, Y.L. Umanskiĭ, Classification of four-dimensional integrable Hamiltonian systems and Poisson actions of  $\mathbb{R}^2$  in extended neighborhoods of simple singular points. II, *Sbornik: Mathematics* **184**/4, 105–138 (1993), doi:[10.1070/SM1994v078n02ABEH003481](https://doi.org/10.1070/SM1994v078n02ABEH003481)
- [20] L.M. Lerman, Y.L. Umanskiĭ, Classification of four-dimensional integrable Hamiltonian systems and Poisson actions of  $\mathbb{R}^2$  in extended neighbourhoods of simple singular points. III. Realization, *Sbornik: Mathematics* **186**/10, 89–102 (1995), doi:[10.1070/SM1995v186n10ABEH000080](https://doi.org/10.1070/SM1995v186n10ABEH000080)
- [21] L.M. Lerman, Y.L. Umanskiĭ, *Four-Dimensional Integrable Hamiltonian Systems with Simple Singular Points (Topological Aspects)*, American Mathematical Society (1998), isbn:[0821803751](https://doi.org/10.1090/S0821803751)
- [22] N.C. Leung, M. Symington, Almost toric symplectic four-manifolds, *Journal of Symplectic Geometry* **8**/2, 143–187 (2010),
- [23] S.V. Manakov, Note on the integration of Euler’s equation of the dynamics of an  $N$  dimensional rigid body, *Functional Analysis and its Applications* **10**/4, 328–329 (1976), doi:[10.1007/BF01076037](https://doi.org/10.1007/BF01076037)
- [24] J. Martinet, *Singularities of smooth functions and maps*, London Mathematical Society Lecture Note Series **58**, Cambridge University Press (1982), isbn:[0521233984](https://doi.org/10.1017/CBO9780511523398)
- [25] N.N. Nekhoroshev, D.A. Sadovskii, B.I. Zhilinskiĭ, Fractional hamiltonian monodromy, *Annales Henri Poincaré* **7**/6, 1099–1211 (2006), doi:[10.1007/s00023-006-0278-4](https://doi.org/10.1007/s00023-006-0278-4)
- [26] D.A. Sadovskii, B.I. Zhilinskiĭ, Quantum monodromy and its generalizations and molecular manifestations, *Molecular Physics* **104**/16, 2595–2615 (2006), doi:[10.1080/00268970600673363](https://doi.org/10.1080/00268970600673363)
- [27] D.A. Sadovskii, B.I. Zhilinskiĭ, Hamiltonian systems with detuned 1:1:2 resonance: Manifestation of bidromy, *Annals of Physics* **322**/1, 164–200 (2007), doi:[10.1016/j.aop.2006.09.011](https://doi.org/10.1016/j.aop.2006.09.011)
- [28] L.N. Sretenskiĭ, On some cases of integrability of the equation of a gyrostat motion, *Doklady Akademii Nauk USSR* **149**, 292–294 (1963),
- [29] H. Waalkens, H.R. Dullin, P.H. Richter, The problem of two fixed centers: bifurcations, actions, monodromy, *Physica D: Nonlinear Phenomena* **196**/3-4, 265–310 (2004), doi:[10.1016/j.physd.2004.05.006](https://doi.org/10.1016/j.physd.2004.05.006)
- [30] N.T. Zung, A note on degenerate corank-one singularities of integrable Hamiltonian systems, *Commentarii Mathematici Helvetici* **75**, 271–283 (2000), doi:[10.1007/PL00000375](https://doi.org/10.1007/PL00000375)

---

<sup>a</sup> University of Groningen  
 Johann Bernoulli Institute for Mathematics and Computer Science  
 PO Box 407  
 9700 AK Groningen The Netherlands  
 E-mail: [konstantinos@efstathiou.gr](mailto:konstantinos@efstathiou.gr)

<sup>b</sup> Università degli Studi di Padova  
 Dipartimento di Matematica  
 Via Trieste 63  
 35121 Padova, Italy  
 E-mail: [giacobbemath@unipd.it](mailto:giacobbemath@unipd.it)